Atmos. Meas. Tech. Discuss., 3, 3319–3344, 2010
www.atmos-meas-tech-discuss.net/3/3319/2010/
doi:10.5194/amtd-3-3319-2010

Atmospheric Measurement Techniques Discussions

Intercomparison of CALIOP and MODIS aerosol optical depth retrievals

C. Kittaka[1,†], D. M. Winker[2], M. A. Vaughan[2], A. Omar[2], and L. A. Remer[3]

[1]Science Systems and Applications Inc., Hampton, VA, USA
[2]NASA Langley Research Center, Hampton, VA, USA
[3]NASA Goddard Spaceflight Center, Greenbelt, MD, USA
[†]deceased

Received: 7 July 2010 – Accepted: 9 July 2010 – Published: 9 August 2010

Correspondence to: D. M. Winker (david.m.winker@nasa.gov)

Published by Copernicus Publications on behalf of the European Geosciences Union.

Abstract

The Cloud-Aerosol Lidar with Orthogonal Polarization (CALIOP) is carried on the CALIPSO satellite and has acquired global aerosol profiles since June 2006. CALIPSO is flown in formation with the Aqua satellite as part of the A-train satellite constellation, so that a large number of coincident aerosol observations are available from CALIOP and the MODIS-Aqua instrument. This study compares column aerosol optical depth at 0.532 µm derived from CALIOP aerosol profiles with MODIS-Aqua 0.55 µm aerosol optical depth over the period June 2006 through August 2008. The study is based on the CALIOP Version 2 Aerosol Layer Product and MODIS Collection 5. While CALIOP is first and foremost a profiling instrument, this comparison of column aerosol optical depth provides insight into quality of CALIOP aerosol data. It is found that daytime aerosol optical depth from the CALIOP Version 2 product has a small global mean bias relative to MODIS Collection 5. Regional biases, of both signs, are larger and biases are seen to vary somewhat with season. In northern mid-latitudes, aerosol optical depth from CALIOP is lower, on average, than from MODIS. This may be partly due to a latitude-dependent calibration error in Version 2 CALIOP Level 1 daytime 0.532 µm profiles. This comparison of CALIOP and MODIS also provides insight into possible biases in the MODIS aerosol optical depth product due to cloud masking and errors in modeling land surface reflectance.

1 Introduction

Aerosols have important effects on Earth's radiation budget through the scattering and absorption of sunlight, as well as through influences on cloud properties through a variety of different physical mechanisms. Aerosols have many different sources, both natural and anthropogenic, and can be transported on hemispheric scales. Limitations in our ability to observe and characterize aerosols globally are responsible in part for the current uncertainties in predicting global climate change (Yu et al., 2006). We have

AMTD

3, 3319–3344, 2010

Title Page
Abstract | Introduction
Conclusions | References
Tables | Figures
◀| |▶
◀ ▶
Back | Close
Full Screen / Esc
Printer-friendly Version
Interactive Discussion

greatly advanced our understanding of aerosol horizontal distributions using satellite observations from sensors such as AVHRR, TOMS, MODIS, and MISR. However, the vertical profile of aerosol still remains uncertain. The CALIPSO satellite was developed to provide a global profiling capability to complement current capabilities to observe aerosol and cloud from space.

The Cloud-Aerosol Lidar with Orthogonal Polarization (CALIOP) instrument, onboard the CALIPSO satellite, provides detection and characterization of aerosols and clouds using profiles of laser depolarization and 2-wavelength laser backscatter. The active laser technique provides high vertical resolution and allows retrievals of aerosol profiles under both cloud-free conditions and above lower-lying clouds. CALIOP has now acquired a four-year record of global aerosol and cloud vertical distributions since June 2006 (Winker et al., 2010). These observations reveal the vertical profile of aerosol on a global basis for the first time. CALIPSO flies as part of the A-Train constellation along with the PARASOL, Aqua, Aura, and Cloudsat satellites (Stephens et al., 2003). The A-train orbit is sun-synchronous, with a 1:30 p.m. orbit crossing time and a 98° inclination.

While the strength of CALIOP is aerosol profile measurements, there are no independent aerosol datasets which can be used to validate CALIOP profiles globally. There are a relatively small number of groundbased lidars suitable for providing data for aerosol validation and the existing systems are far from ideally located for providing measurements of important aerosol source regions. Field campaigns involving airborne lidars are useful, but provide very limited spatial and temporal coverage. Aerosol optical depth (AOD) data from MODIS-Aqua can be compared with AOD derived from CALIOP daytime profiles of aerosol extinction. While this is less than ideal, the MODIS Collection 5 AOD product has undergone extensive validation and data quality is well understood, and flying the CALIPSO and Aqua satellites in formation provides a large number of near-simultaneous, coincident aerosol observations with global coverage. Comparisons of AOD from MODIS and CALIOP characterize the CALIOP AOD product and also provide valuable insights into the performance of the CALIOP profile retrievals.

AMTD
3, 3319–3344, 2010

Further investigation can identify sources of error in the CALIOP retrievals.

AOD at 0.532 µm derived from the CALIOP Version 2.01 5-km Aerosol Layer Product has been compared with AOD at 0.55 µm from MODIS-Aqua Collection 5. This paper presents an initial, statistical comparison, which illuminates characteristics of the CALIOP Version 2.01 AOD product and also serves as a benchmark against which to compare the CALIOP Version 3 product. Other validation studies are underway, utilizing AOD measurements from AERONET and direct aerosol extinction profile measurements from airborne HSRL operated by NASA Langley Research Center (Hair et al., 2009). These studies will provide additional perspectives on CALIOP AOD data quality.

2 Measurements

Since the launch of the MODIS and MISR instruments in 1999, advanced satellite measurements have greatly increased our knowledge of the global distribution and properties of aerosols (Kaufman et al., 2002). MODIS provides daily near-global coverage and retrievals of AOD at several wavelengths over both ocean and land. Relative to previous satellite sensors used to retrieve aerosol, MODIS provided improved spatial resolution (500 m), better spectral coverage, and improved calibration. Development of the AERONET network of groundbased sunphotometers has allowed an unprecedented degree of validation of aerosol retrievals from MODIS.

CALIOP, acquiring global aerosol observations since 2006, is complementary to MODIS in several ways. While CALIOP has a swath with essentially zero width, observing only along the sub-satellite point it acquires vertical profiles at two wavelengths (0.532 µm and 1.064 µm) and two orthogonal polarizations, with a vertical resolution of 30–60 m (Hunt et al., 2009). Analysis of the spectral and polarization diversity of the return signals, as a function of altitude, provides some skill in identifying aerosol type and also allows identification of columns which are inhomogeneous in terms of aerosol type (Omar et al., 2009). While the MODIS and CALIOP retrievals rely on

AMTD
3, 3319–3344, 2010

several assumptions and are subject to several sources of error, the retrieval methods are completely different and the CALIOP assumptions and sources of error are independent of those of MODIS. Thus, a comparison of the two AOD datasets can lead to insights into the strengths and limitations of both datasets.

2.1 MODIS

The Moderate Resolution Imaging Spectroradiometer (MODIS) on the Aqua satellite measures scattered radiances at 36 wavelengths from 0.41 to 14 µm. A 2330-km swath provides near-global coverage every day. Different algorithms are used to retrieve AOD over ocean and over land. Over ocean, seven wavelengths (0.47, 0.55, 0.66, 0.86, 1.2, 1.6, and 2.12 µm) are used to retrieve aerosol optical depth and other aerosol properties (Tanré et al., 1997). These channels have spatial resolutions of 250 m or 500 m and calibration of the radiances is believed to be accurate to 2% or better. Radiances are grouped into nominal 10-km cells containing 20 × 20 pixels at 500-m resolution. All 400 pixels must be identified as ocean pixels for the ocean algorithm to be applied. If any land is contained within the cell the land algorithm is applied (Remer et al., 2005). After screening for clouds and marine sediments, the brightest 25% and darkest 25% of the remaining 500-m pixels are discarded. Retrievals are performed on the remaining pixels. To avoid errors due to sunglint, retrievals are performed only for pixels where the glint angle is greater than 40°. Outside the glint regions the water-leaving radiance is assumed to be negligible except at 550 nm where the surface reflectance is assumed to be 0.005. Wind speed is assumed to be 6 m/s everywhere.

Over land, AOD is retrieved at 0.47, 0.55, and 0.66 µm (Kaufman et al., 1997). As described above, the land algorithm is also used in coastal areas. The land algorithm only retrieves AOD over dark surfaces. Pixels containing snow/ice and cloudy pixels are masked out. Cloud mask quality flags (cf_land, cf_ocean) are included in the data product to indicate the fraction of cloudy pixels within the 10 × 10 km^2 grid cells. cf_x = 3 indicates greater than 90% cloudy pixels, while cf_x = 0 indicates fewer than 30% cloud pixels. After masking, dark pixels are selected based on their reflectance at 2.12 µm.

AMTD
3, 3319–3344, 2010

Surface reflectance must fall within the range 0.01 to 0.25 to be selected. Pixels are then sorted according to their reflectance at 0.66 µm and the darkest 20% and brightest 50% within each 10-km cell are discarded. Retrievals are performed on the remaining 30% of pixels.

A number of validation studies have characterized uncertainties of the MODIS AOD product. Relative to AERONET AOD measurements, Remer et al. (2005) found that one standard deviation of MODIS-Terra AOD fell within the expected uncertainties of $\Delta\tau = \pm 0.03 \pm 0.05\tau$ over ocean and $\Delta\tau = \pm 0.05 \pm 0.15\tau$ over land. Ichoku et al. (2005) compared AOD from MODIS-Terra and MODIS-Aqua averaged over $50 \times 50\,km^2$ boxes with Aeronet AOD. Redemann et al. (2006) compared MODIS AOD at the $10 \times 10\,km^2$ scale of the Level 2 product with AERONET. Kahn et al. (2007) look at sources of systematic bias in AOD retrievals over the ocean from the MODIS and MISR instruments on the Terra satellite.

2.2 CALIOP

CALIOP measures elastic laser backscatter at 1.064 µm and the parallel and cross-polarized components of the 0.532 µm return signal, from which the linear depolarization is derived (Hunt et al., 2009). At the Earth's surface, the diameter of the laser footprint is 70 m, with successive footprints spaced by 333 m along the orbit track. The instrument has a fixed near-nadir view angle, so the measurements map a vertical curtain along the orbital path. The 0.532 µm backscatter signal is sampled every 30 m vertically from −0.5 km to 8.2 km. Between 8.2 km and 20.2 km altitude profiles are averaged to 60 m in the vertical and every three successive shots are averaged together to give a horizontal resolution of 1 km. The geolocated and altitude-registered Level 1 data are calibrated before being processed for Level 2 data products. Daytime measurements have a lower signal-to-noise ratio than at night owing to the noise added by the solar background illumination. Subtle diurnal differences in retrievals are caused by the use of different calibration algorithms for day and for night. Briefly, extinction is retrieved in three steps: (1) backscatter profiles are searched for layers with horizontal

AMTD
3, 3319–3344, 2010

averaging varying from 1/3 km to 80 km; (2) identified layers are classified as cloud or aerosol; and (3) aerosol and cloud extinction profiles are retrieved, starting with the highest layers detected and working down to the Earth's surface (Winker et al., 2009 and references therein). Aerosol retrievals are performed on layers which have been horizontally averaged over 5 km, 20 km, or 80 km. Retrieval results are reported at 5-km horizontal scale in the 5-km Aerosol Layer Product. Retrieval results from 20-km or 80-km layers are repeated 4 times, or 16 times, in the 5-km product.

Extinction retrieval from a backscatter lidar such as CALIOP is under-determined and an additional constraint is required. When the layer transmittance can be accurately measured, from clear-air signals on either side of a layer, the measured transmittance yields the layer optical depth directly and can be used as a constraint on the extinction retrieval (Young, 1995). This occurs rarely during daytime, when the SNR of clear-air returns is lower than at night. Therefore, an algorithm is used to estimate the "lidar ratio" (the ratio of particle extinction to 180-degree backscatter) from the 0.532 µm backscatter and depolarization signals (Omar et al., 2009), which provides the necessary constraint for the retrieval. Aerosol extinction is retrieved above clouds and below optically thin clouds, as well as in cloudfree columns, but only within identified aerosol layers (Young and Vaughan, 2009).

The primary products used in this paper are the 0.55 µm Optical_Depth_Land_and_Ocean from the MODIS-Aqua Level 2 aerosol data product (MYD04_L2), and the Feature_Optical_Depth_532 from the CALIOP Level 2 5-km Aerosol Layer Product. Feature_Optical_Depth is summed over each aerosol layer in a 5-km the column to obtain the column AOD.

Figure 1 shows seasonally-averaged AOD from MODIS and from CALIOP observations, plotted on the same 5 × 5 degree equal-angle grid. Daytime and nighttime AOD distributions from CALIOP are generally similar. Differences are due to a combination of differences between day and night sensitivity, differences in systematic calibration errors for day and night, differences in spatial sampling, and diurnal changes in the aerosol. Even though the MODIS and daytime CALIOP observations are simultane-

AMTD
3, 3319–3344, 2010

ous, a number of differences can be seen, due in part to differences in sampling of the two instruments. CALIOP retrieves AOD over the Sahara desert and other bright surfaces where the MODIS product has no data. Daytime CALIOP measurements extend to higher southern latitudes than MODIS. Because CALIOP measurements are at nadir only, many fewer samples are acquired than from MODIS and many grid cells are sampled only about once per week, causing CALIOP AOD to appear to be noisier than MODIS AOD. Intense but intermittent aerosol events – such as dust storms or forest fires – may be missed by CALIOP, resulting in smaller grid-cell averages than MODIS AOD which better represents the seasonal-mean AOD at smaller spatial scales due to its daily coverage.

3 Method

Because of the large differences in spatial sampling, the remainder of the comparisons in this paper will be based on simultaneous, co-located daytime CALIOP and MODIS observations. The comparison of matched observations reduces uncertainties from spatial and temporal differences of the observations, but greatly reduces the number of observations and so may compromise the geophysical representivity. First, MODIS 10-km cells coincident with CALIOP 5-km pixels are identified. After applying quality screening to the CALIOP aerosol data, layer optical depths are summed to derive 0.532 µm column AOD. Coincident CALIOP and MODIS AOD are then stored, along with cloud masking information.

3.1 Sampling geometry and co-location

CALIOP laser footprints have a diameter of 70 m with a center-center separation of about 330 m. Thus there are about 30 footprints within the $10 \times 10\,\mathrm{km}^2$ MODIS Level 2 cell. The orbits of the CALIPSO and Aqua satellites are controlled to keep the along-track separation at about 2 min and the relative cross-track error of the two satellite

AMTD
3, 3319–3344, 2010

groundtracks to about 10 km. MODIS AOD is not retrieved for pixels over water where the sunglint angle is less than 40°. Therefore the CALIPSO orbit was shifted relative to the Aqua orbit to minimize the occurrence of MODIS sunglint at the CALIOP footprint. On the day side of the orbit at the equator the CALIPSO subsatellite point falls 215 km to the east of the Aqua subsatellite point. At the orbit turning points (82° N and 82° S) the cross-track bias is zero and increases to 215 km at the equator. Thus the CALIOP footprint is continually moving cross-track with respect to the MODIS 10 × 10 km^2 grid (Fig. 2). Spatially coincident CALIOP and MODIS AOD observations are identified when the distance between the center of a CALIPSO 5-km "pixel" and that of a MODIS pixel is less than 10 km. This criterion automatically selects time-coincident measurements (within 2 min).

3.2 Data screening

Additional quality screening is applied to CALIOP Level 2 aerosol data before use. In a small number of cases, the initial lidar ratio is automatically reduced to avoid a diverging solution (Winker et al., 2009). It has been found that these retrievals are not reliable, so columns containing aerosol layers where the final lidar ratio is different from the initial lidar ratio are screened out. Also, in Version 2 data, a small number of aerosol layers are found to have anomalously large layer-integrated attenuated backscatter values, most often due to overcorrection of the attenuation of overlying layers. Therefore, columns containing aerosol layers with integrated attenuated backscatter greater than 0.01 sr^{-1} are also screened out.

Figure 4 shows the number of 5-km CALIOP columns with valid data from both instruments between 15 June 2006 and 31 August 2008. For MODIS this represents all of the pixels except for those filled with a missing value due to cloud cover, high reflectance surface, or sunglint, while the CALIPSO pixels with valid data are those remaining after the screening described above. Over this time period there are about 1.8 million coincident AOD retrievals. Over ocean, about 12% of the CALIPSO daytime footprints have a coincident MODIS AOD value. The co-located measurements

AMTD
3, 3319–3344, 2010

are heavily weighted toward the Southern Hemisphere due to a combination of cloud cover, reflective land surfaces, and sunglint. Even with the 215 km offset, the CALIPSO ground track falls just within the edge of the MODIS sun glint areas at northern mid-latitudes from May through July. This contributes to fewer coincident samples over the ocean in the Northern Hemisphere spring and summer. In Collection 5, AOD is not retrieved over highly reflective land surfaces such as ice/snow and deserts, which reduces the number of coincidences over land at mid and high latitudes. Polar night further reduces the number of MODIS observations at high latitudes and there are relatively few coincident samples in the tropics due to frequent cloud cover.

4 Effects of cloud screening

The next few figures show the frequency distributions of AOD values from the two instruments. These distributions are used to help identify general characteristics of the two data sets and determine the effects of additional screening. Figure 5 shows the two-dimensional frequency distributions of the coincident CALIOP and MODIS AOD values over ocean (a) and over land (b) for the time period from 15 June 2006 to 31 August 2008. The samples going into these histograms are instantaneous, co-located MODIS and CALIOP AOD values. The CALIOP AOD data are screened using the method described in the Sect. 3.2, while MODIS AOD is used regardless of cloud fraction within the 10-km cell.

Several features of these plots give insight into data quality. MODIS and CALIOP AOD over ocean are somewhat correlated, although the scatter is very large. There is little correlation over land however. CALIOP uses the same retrieval algorithm over land and ocean. The difference between Fig. 5a and b may be due to larger instantaneous uncertainties in the MODIS land algorithm, or may just reflect the higher spatial variability of aerosol over land. Looking at AOD values smaller than 0.2, CALIOP AOD is biased somewhat low relative to MODIS for both land and ocean. A prominent feature seen in both scatter plots is a high population in the MODIS AOD bins between

AMTD
3, 3319–3344, 2010

zero and 0.6 for zero CALIOP AOD. This feature extends to −0.05 in the MODIS bins for land. A similar feature is seen over land for zero MODIS AOD and CALIOP AOD less than 0.1. A noticeable feature in the ocean plot is an enhanced population in the CALIOP AOD range between 0.4 and 0.8 for MODIS AOD smaller than 0.2.

The scatter plots in Fig. 6 are produced the same as those in Fig. 5 except for more stringent cloud screening, using only coincident AOD from grid cells where less than 30% of the pixels are cloudy ($cf\_x = 0$). The area of enhanced CALIOP AOD between 0.4 and 0.8 corresponding to MODIS AOD less than 0.2, seen in Fig. 5a, has disappeared. When the locations of this population are mapped, they are seen to predominantly come from relatively clean ocean regions dominated by trade cumulus, and analysis of CALIOP cloud height data shows the population is associated with clouds having tops below 2 km. Therefore, this population may be an artifact due to a programming error in the CALIOP Version 2 production software where small-scale boundary layer clouds are not properly cleared from 5-km average profiles. These cloud contaminated profiles are most often classified as cloud, but if classified as aerosol they would tend contribute to a high bias in AOD. Figure 6a also shows substantial effects of the additional cloud screening on the population of MODIS bins for zero CALIOP AOD over ocean. The frequency of large MODIS AOD values is greatly reduced, indicating these may be due to cloud contamination or possibly side-scattering from clouds. The distribution for land, however, exhibits little change in the general pattern with the exception of the high MODIS AOD range.

One additional level of cloud-screening was applied. CALIOP identifies clouds in roughly 20–30% of MODIS $10 \times 10\,km^2$ grid cells with less than 30% cloudy pixels. The histograms of Fig. 6 don't change significantly if these cloudy columns are screened out, but the mean AOD decreases somewhat. Table 1 summarizes changes in mean AOD for the three different levels of cloud screening.

The large MODIS AOD values corresponding to near-zero CALIOP AOD – seen along the x-axis of Figs. 5b and 6b – are not significantly affected by more stringent cloud screening. If we map the location of these observations, many are associated

AMTD
3, 3319–3344, 2010

with arid regions having 2.12 µm surface reflectance greater than 15% (Fig. 7). While there are a number of possible explanations for high MODIS AOD and near-zero CALIOP AOD, it is likely that use of incorrect surface reflectivity values in the MODIS retrievals is one source.

5 Comparison of spatial averages

The following analyses are based on fully cloud-screened data, where fewer than 30% of MODIS pixels are cloudy and CALIOP detects no clouds in the column. Figure 7 compares MODIS and CALIOP zonal mean AOD distributions for ocean and for land, averaged over the entire 27-month period. Only data passing the most stringent cloud screening has been used: MODIS flag cf = 0 and no cloud identified by CALIOP. Over the ocean, zonal mean AOD differences (MODIS–CALIPSO) range from −0.02 to +0.06. The agreement is reasonably good, except that MODIS AOD is significantly larger than CALIOP north of 30° N and about 0.03 larger than CALIOP between 40°–60° S. The range of the AOD difference over land is much larger, from −0.14 to +0.18, which may be due in part to the much smaller number of co-located samples over land. Referring back to Fig. 4, it can be seen that many land regions have few co-located samples relative to much of the ocean. CALIOP AOD is lower than MODIS at high northern and southern mid-latitudes, as over ocean, but is also higher than MODIS between 20° S–20° N, a region which is likely dominated by smoke from biomass fires. There is a known Northern Hemisphere bias in the Version 2 daytime CALIOP 0.532 µm calibration. The calibration bias causes the attenuated backscatter signal to be low in northern mid-latitudes and may contribute to the generally smaller CALIOP AOD values seen in the Northern Hemisphere in Fig. 8.

To provide more insight into these zonal patterns, Fig. 9 illustrates the geographical distribution of seasonally-averaged differences in co-located MODIS and CALIOP AOD. Only CALIOP AOD from cloud-free 5-km columns and MODIS AOD from grid cells with less than 30% cloud pixels are used. Retrievals over surfaces flagged as snow/ice are also screened out. A 5° × 5° grid is used to provide sufficient statistics for the nadir-only CALIPSO retrievals without losing regional patterns of the AOD distribution. A strong hemispheric pattern is seen, with MODIS AOD tending to be higher than CALIOP AOD in the northern and somewhat lower in the Southern Hemisphere, except for 40°–60° S during Austral spring and summer when MODIS AOD is somewhat higher. The magnitude of AOD differences is considerably larger over land than that over ocean, partly because mean AOD tends to be larger over land than over ocean.

Numerous regional biases can also be seen, some which are counter to the overall north-south pattern. MODIS AOD is consistently lower than CALIOP over India, except in arid northwest India and Pakistan where MODIS is consistently higher. In this comparison, CALIOP tends to be higher than MODIS over the eastern US and lower over Western US. CALIOP AOD is generally larger than MODIS over tropical Africa, except during DJF where MODIS AOD is larger over Niger/Nigeria. In the Southern Hemisphere, CALIOP AOD is consistently higher over central and southern Africa, while MODIS is consistently higher in the Gulf of Guinea – both regions typically dominated by smoke. MODIS AOD is consistently higher in southern Argentina. The seasonal cycle over Brazil is not well sampled, probably because of persistent cloud cover. During the dry season (SON) CALIOP AOD is higher in eastern Brazil, while MODIS AOD is significantly higher in western Brazil and Bolivia. There is a degree of consistency in these regional differences, pointing to the likelihood of underlying causes in algorithms and calibration.

6 Summary

This paper has developed a methodology for screening CALIOP AOD data and comparing with MODIS AOD. Initial AOD comparisons have been performed based on CALIOP Version 2 and MODIS Collection 5 data. These comparisons show that global mean AOD from CALIOP is somewhat low relative to MODIS-Aqua, but that there are significant regional biases of both signs. The work reported here forms a basis for

AMTD
3, 3319–3344, 2010

further comparisons using the recently released CALIOP Version 3 data. Apparent systematic regional differences identified here, such as between southern Africa and the Gulf of Guinea, or between eastern and western United States, provide motivation for more detailed case studies to diagnose the source of these differences at the algorithm level.

References

Hair, J. W., Hostetler, C. A., Cook, A., Harper, D. B., Ferrare, R., Mack, T. L., Welch, W., Ramos Isquierdo, L., and Hovis, F.: Airborne High Spectral Resolution Lidar for Profiling Aerosol Optical Properties, Appl. Opt., 47, 6734–6752, 2008.

Hunt, W. H., Winker, D. M., Vaughan, M. A., Powell, K. A., Lucker, P. L., and Weimer, C.: CALIPSO Lidar Description and Performance Assessment, J. Atmos. Oceanic Technol., 26, 1214–1228, 2009.

Ichoku, C., Chu, D. A., Mattoo, S., Kaufman, Y. J., Remer, L. A., Tanré, D. Slutsker, I., and Holben, B. N.: A spatio-temporal approach for global validation and analysis of MODIS aerosol products, Geophys. Res. Lett., 29, L8006, doi:10.1029/2001GL013206, 2002.

Kahn, R. A., Garay, M. J., Nelson, D. L., Yau, K. K., Bull, M. A., Gaitley, B. J., Martonchik, J. V., and Levy, R. C.: Satellite-derived aerosol optical depth over dark water from MISR and MODIS: comparisons with AERONET and implications for climatological studies, J. Geophys. Res., 112, D18205, doi:10.10.1029/2006JD008175, 2007.

Kaufman, Y., Tanré, D., and Boucher, O.: A satellite view of aerosols in the climate system, Nature, 419, 215–223, 2002.

Kaufman, Y. J., Tanré, D., Remer, L. A., Vermote, E. F., Chu, A., and Holben, B. N.: Operational remote sensing of tropospheric aerosol over land from EOS moderate resolution imaging spectroradiometer, J. Geophys. Res., 102, 17051–17067, 1997.

Levy, R. C., Remer, L. A., Kaufman, Y. J., Tanré, D., Mattoo, S., Vermote, E., and Dubovik, O.: Revised Algorithm Theoretical Basis Document: MODIS Aerosol Products MOD/MYD04, 2006.

Liu, Z., Vaughan, M. A., Winker, D. M., Kittaka, C., Kuehn, R. E., Getzewich, B. J., Trepte, C. R., and Hostetler, C. A.: The CALIPSO Lidar Cloud and Aerosol Discrimination: Version 2

AMTD

3, 3319–3344, 2010

Algorithm and Initial Assessment of Performance, J. Atmos. Oceanic Technol., 26, 1198–1213, doi:10.1175/2009JTECHA1229.1, 2009.

Omar, A., Winker, D., Kittaka, C., Vaughan, M., Liu, Z., Hu, Y., Trepte, C., Rogers, R., Ferrare, R., Kuehn, R., and Hostetler, C.: The CALIPSO Automated Aerosol Classification and Lidar Ratio Selection Algorithm, J. Atmos. Oceanic Technol., 26, 1994–2014, doi:10.1175/2009JTECHA1231.1, 2009.

Redemann, J., Zhang, Q., Schmid, B., Russell, P. B., Livingston, J. M., Jonsson, H., and Remer, L. A.: Assessment of MODIS-derived visible and near-IR aerosol optical properties and their spatial variability in the presence of mineral dust, Geophys. Res. Lett., 33, L18814, doi:10.1029/2006GL026626, 2006.

Remer, L. A., Kaufman, Y. J., Tanré, D., Mattoo, S., Chu, D. A., Martins, J. V., Li, R.-R., Ichoku, C., Levy, R. C., Kleidman, R. G., Eck, T. F., Vermote, E., and Holben, B. N.: The MODIS Aerosol Algorithm, Products, and Validation, J. Atmos. Sci., 62, 947–973, 2005.

Stephens, G. L., Vane, D. G., Boain, R. J., Mace, G. G., et al.: The CloudSat mission and the A-Train: A new dimension of space-based observations of clouds and precipitation, B. Am. Meteorol. Soc., 83, 1771–1790, 2002.

Tanré, D., Kaufman, Y. J., Herman, M., and Mattoo, S.: Remote sensing of aerosol properties over oceans using the MODIS/ESO spectral radiances, J. Geophys. Res., 102, 16971–16988, 1997.

Vaughan, M., Powell, K., Kuehn, R., Young, S., Winker, D., Hostetler, C., Hunt, W., Liu, Z., McGill, M., and Getzewich, B.: Fully Automated Detection of Cloud and Aerosol Layers in the CALIPSO Lidar Measurements, J. Atmos. Ocean. Technol., 26, 2034–2050, 2009.

Winker, D. M., Pelon, J., Coakley, J. A., Ackerman, S. A., et al.: The CALIPSO Mission: a Global 3-D View of Aerosols and Clouds, B. Am. Meteorol. Soc., 91, August 2010, in press.

Winker, D. M., Vaughan, M. A., Omar, A., Hu, Y., Powell, K. A., Liu, Z., Hunt, W. H., and Young, S. A.: Overview of the CALIPSO mission and CALIOP data processing algorithms, J. Atmos. Ocean Tech., 26, 2310–2323, doi:10.1175/2009JTECHA1281, 2009.

Young, S. A.: Analysis of lidar backscatter profiles in optically thin clouds, Appl. Opt., 34, 7019–7031, 1995.

Young, S. A. and Vaughan, M. A.: The retrieval of profiles of particulate extinction from Cloud Aerosol Lidar Infrared Pathfinder Satellite Observations (CALIPSO) data: Algorithm description, J. Atmos. Oceanic Technol., 26, 1105–1119, doi:10.1175/2008 JTECHA1221.1, 2009.

AMTD

3, 3319–3344, 2010

Yu, H., Kaufman, Y. J., Chin, M., Feingold, G., Remer, L. A., Anderson, T. L., Balkanski, Y., Bellouin, N., Boucher, O., Christopher, S., DeCola, P., Kahn, R., Koch, D., Loeb, N., Reddy, M. S., Schulz, M., Takemura, T., and Zhou, M.: A review of measurement-based assessments of the aerosol direct radiative effect and forcing, Atmos. Chem. Phys., 6, 613–666, doi:10.5194/acp-6-613-2006, 2006.

AMTD
3, 3319–3344, 2010

Table 1. Global-mean AOD for different cloud-screening criteria. Averaging period is JJA between 15 June 2006 and 31 August 2008.

	Ocean		Land	
	MODIS	CALIOP	MODIS	CALIOP
All MODIS AOD	0.120	0.084	0.145	0.089
MODIS < 30% cloudy	0.096	0.082	0.126	0.102
CALIOP cloud-free	0.083	0.076	0.082	0.094

AMTD
3, 3319–3344, 2010

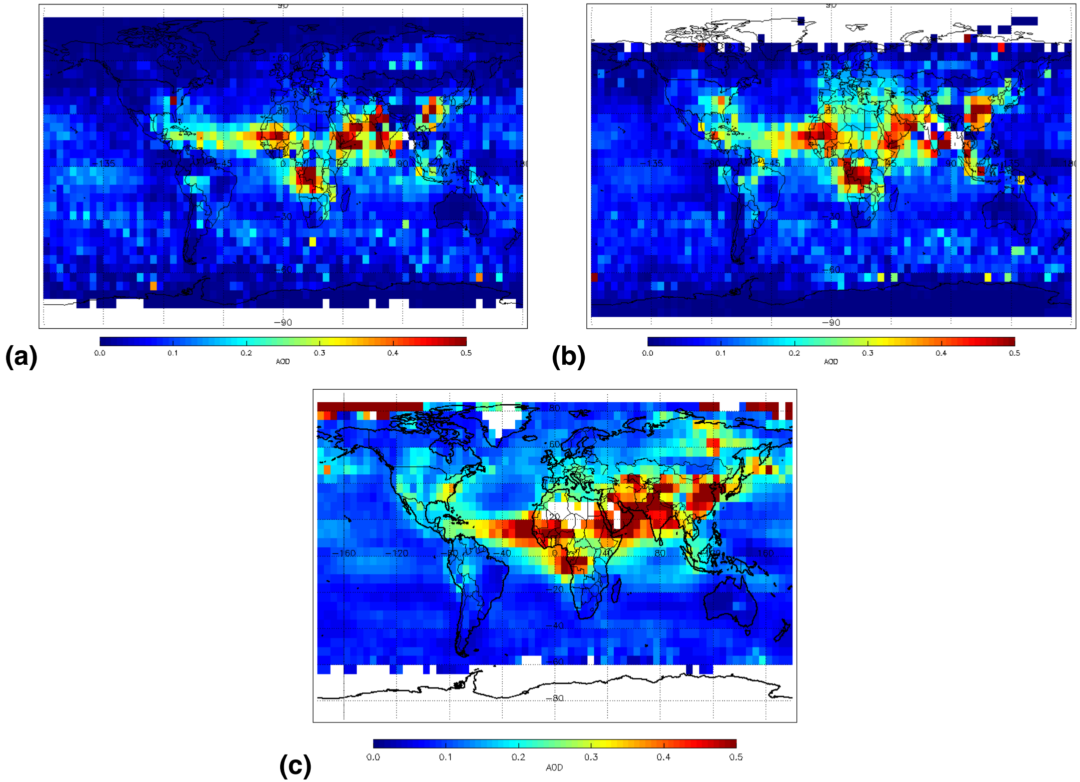

Fig. 1. Seasonal-mean AOD distributions for JJA 2006 from **(a)** CALIOP daytime retrievals; **(b)** CALIOP nighttime retrievals; and **(c)** MODIS retrievals.

AMTD
3, 3319–3344, 2010
Intercomparison of CALIOP and MODIS aerosol optical depth retrievals
C. Kittaka et al.

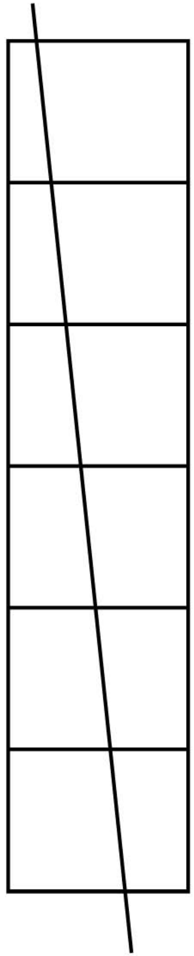

Fig. 2. Geometry of the MODIS 10-km grid vs. the CALIOP "swath".

AMTD

3, 3319–3344, 2010

Intercomparison of CALIOP and MODIS aerosol optical depth retrievals

C. Kittaka et al.

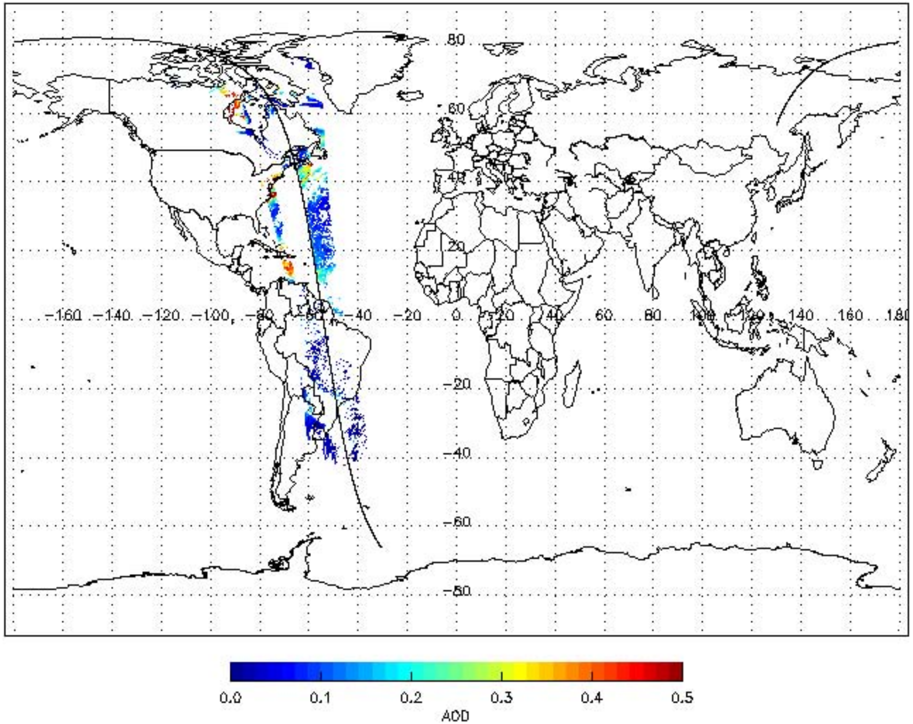

Fig. 3. CALIPSO ground-track superimposed on color-coded MODIS AOD retrievals, 1 July 2006. In northern mid-latitudes, the CALIPSO groundtrack falls within the eastern edge of the MODIS sunglint region, so MODIS AOD is not retrieved to the west of the CALIPSO ground-track.

AMTD
3, 3319–3344, 2010

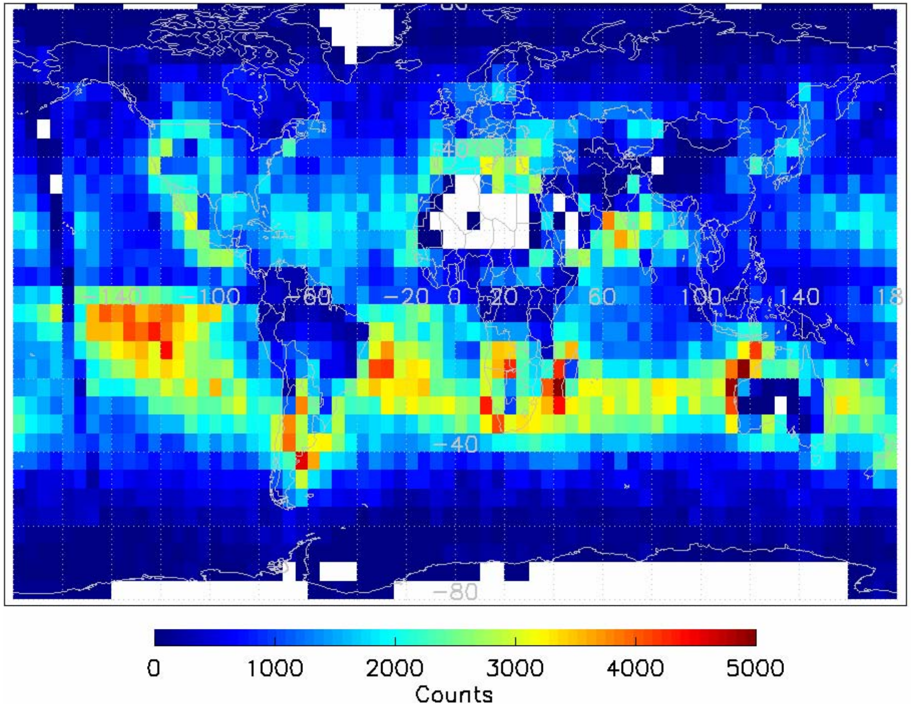

Fig. 4. Map of the number of the CALIPSO and MODIS coincidences with valid AOD data from both instruments from 15 June 2006 to 31 August 2008.

Discussion Paper | Discussion Paper | Discussion Paper | Discussion Paper |

AMTD

3, 3319–3344, 2010

Intercomparison of CALIOP and MODIS aerosol optical depth retrievals

C. Kittaka et al.

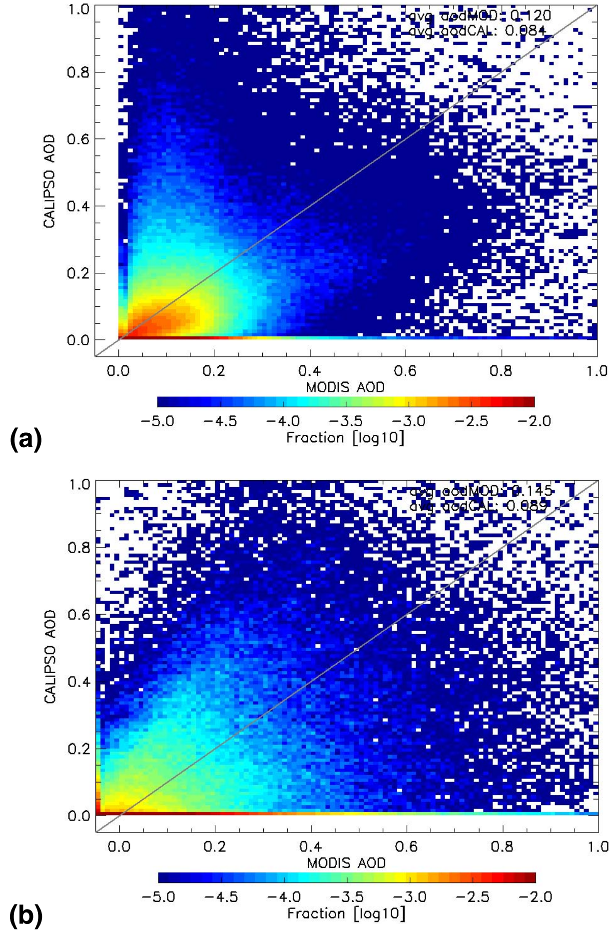

Fig. 5. Frequency distributions of AOD values for JJA (between 15 June 2006 and 31 August 2008) over the global ocean **(a)** and land **(b)** using all coincident CALIOP and MODIS data.

AMTD
3, 3319–3344, 2010

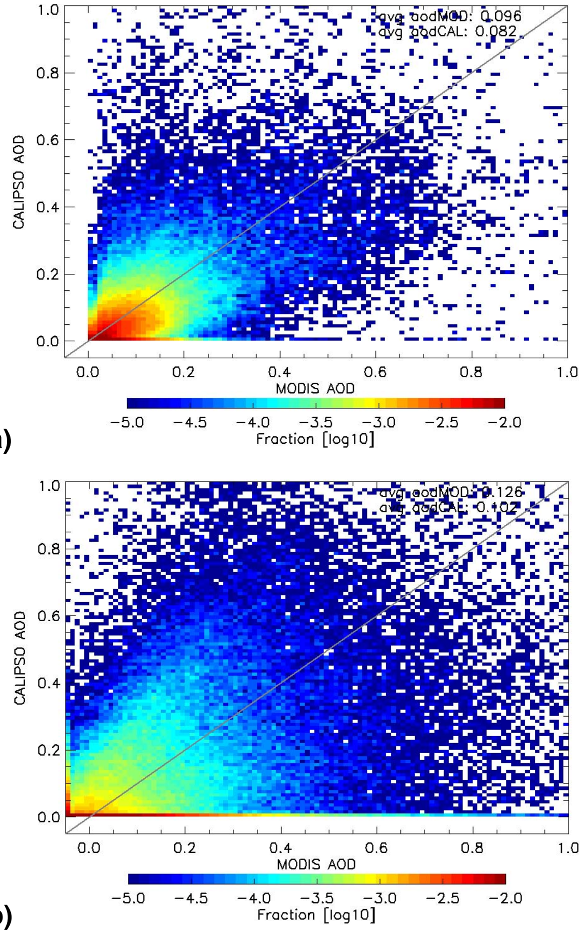

(a) **(b)**

Fig. 6. Frequency distributions of AOD values for JJA (between 15 June 2006 and 31 August 2008) over the global ocean **(a)** and land **(b)** using the most stringent MODIS cloud screening.

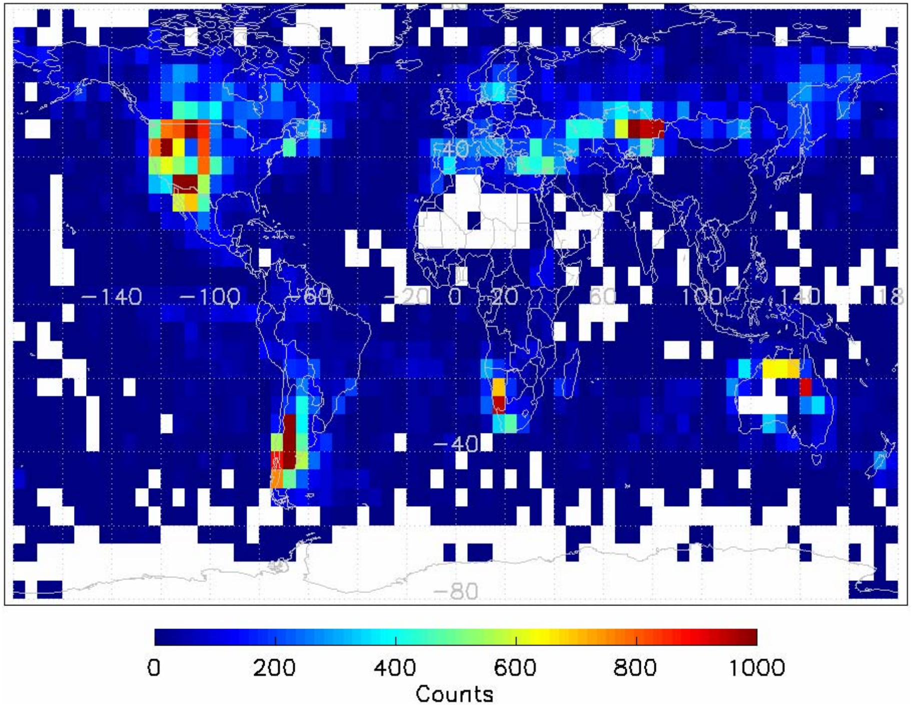

Fig. 7. Number of cloudfree 5-km pixels where CALIOP AOD = 0 and MODIS AOD > 0.05 for instantaneous, co-located retrievals, 15 June 2006–31 August 2008.

AMTD

3, 3319–3344, 2010

Intercomparison of CALIOP and MODIS aerosol optical depth retrievals

C. Kittaka et al.

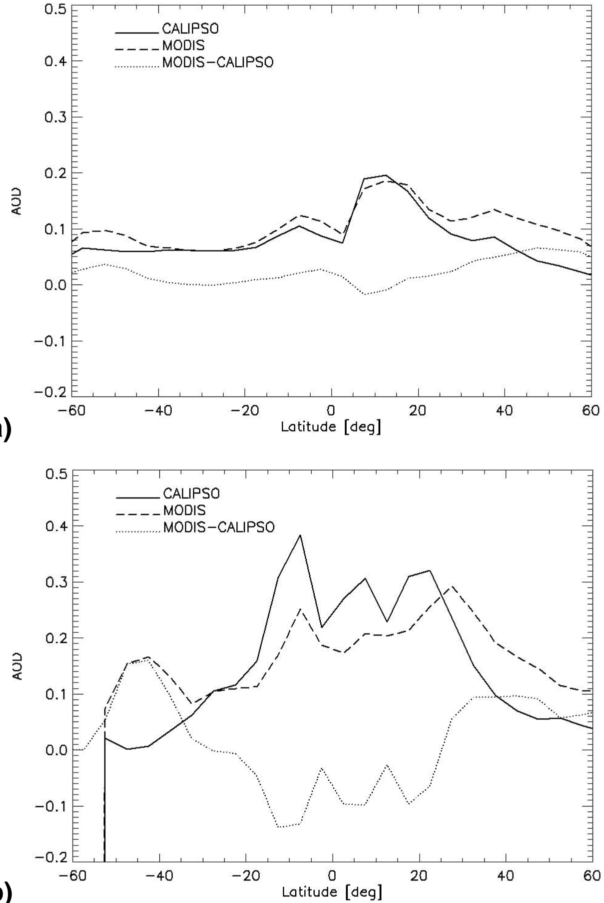

(a)

(b)

Fig. 8. Zonal mean AOD from CALIPSO and from MODIS, and zonal mean MODIS-CALIPSO differences for cloud-free columns for the period 15 June 2006 to 31 August 2008. **(a)** over ocean; **(b)** over land.

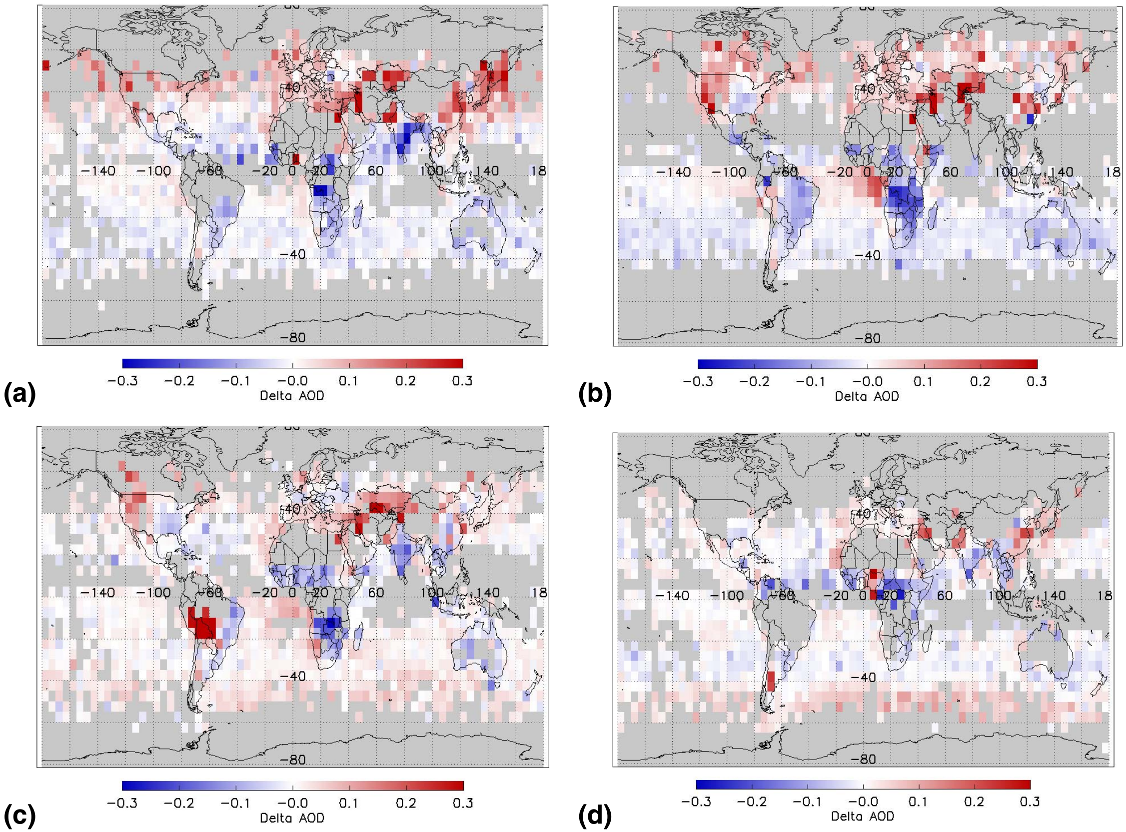

Fig. 9. Seasonal-mean differences of MODIS and CALIOP AOD (MODIS–CALIOP), averaged for seasons over the period of 15 June 2006 to 31 August 2008. Grey indicates grid cells with insufficient number of samples. **(a)** March-April-May; **(b)** June-July-August; **(c)** September-October-November; **(d)** December-January-February.

AMTD
3, 3319–3344, 2010